 DOI: 10.1002/eji.201646758 Eur. J. Immunol. 2017. 47: 504–515

Basic

European Journal of Immunology

Molecular immunology and signaling

Research Article

Functional and structural characterization of four mouse monoclonal antibodies to complement C3 with potential therapeutic and diagnostic applications

Marta Subías Hidalgo[*1,2], *Hugo Yébenes*[*1], *César Rodríguez-Gallego*[*1], *Adrián Martín-Ambrosio*[1,2], *Mercedes Domínguez*[3], *Agustin Tortajada*[1,2], *Santiago Rodríguez de Córdoba*[†1,2] *and Oscar Llorca*[†1]

[1] Centro de Investigaciones Biológicas, Consejo Superior de Investigaciones Científicas, Madrid, Spain
[2] Centro de Investigación Biomédica en Enfermedades Raras, Madrid, Spain
[3] Servicio de Inmunología Microbiana, Centro Nacional de Microbiología, Instituto de Investigación Carlos III Madrid, Spain

C3 is the central component of the complement system. Upon activation, C3 sequentially generates various proteolytic fragments, C3a, C3b, iC3b, C3dg, each of them exposing novel surfaces, which are sites of interaction with other proteins. C3 and its fragments are therapeutic targets and markers of complement activation. We report the structural and functional characterization of four monoclonal antibodies (mAbs) generated by immunizing C3-deficient mice with a mixture of human C3b, iC3b and C3dg fragments, and discuss their potential applications. This collection includes three mAbs interacting with native C3 and inhibiting AP complement activation; two of them by blocking the cleavage of C3 by the AP C3-converase and one by impeding formation of the AP C3-convertase. The interaction sites of these mAbs in the target molecules were determined by resolving the structures of Fab fragments bound to C3b and/or iC3b using electron microscopy. A fourth mAb specifically recognizes the iC3b, C3dg, and C3d fragments. It binds to an evolutionary-conserved neoepitope generated after C3b cleavage by FI, detecting iC3b/C3dg deposition over opsonized surfaces by flow cytometry and immunohistochemistry in human and other species. Because well-characterized anti-complement mAbs are uncommon, the mAbs reported here may offer interesting therapeutic and diagnostic opportunities.

Keywords: Complement inhibition · C3 · C3b · C3bBb convertase · Monoclonal antibody

Additional supporting information may be found in the online version of this article at the publisher's web-site

Introduction

Complement is an essential component of innate immunity and one of the major triggers of inflammatory responses. It plays a crucial role in microbial killing, apoptotic cell clearance, immune complex handling, and modulation of adaptive immune responses [1, 2]. Complement is initiated by three activation pathways, the classical pathway (CP), the lectin pathway (LP), and the alternative pathway (AP). The critical step in these activation pathways is the formation of labile protease complexes, termed C3-convertases (C3bBb in the AP; C4b2a in the CP/LP) that cleave C3 to generate the active fragment, C3b. When C3b is generated, a reactive thioester is exposed which permits covalent binding of C3b to hydroxyl or primary amine groups on the activating surface. C3b

Correspondence: Prof. Oscar Llorca
e-mail: ollorca@cib.csic.es; srdecordoba@cib.csic.es

*Shared first authorship.
†Shared last authorship.

Table 1. Characterization of the anti-C3 mAbs

mAbs	Isotype	Fragment recognition	Domain recognition	KD(M)	Ka ($M^{-1}*s^{-1}$)	Kd(s^{-1})	Functional impact on C3
C3-16.4	IgG1	C3b, iC3b, C3c	MG2, MG6	1.2 nM	$3.7*10^{+4}$	$4.4*10^{-5}$	Blocks AP C3-convertase formation
C3-12.17	IgG2a	C3b, iC3b, C3c	MG3, MG4	63 nM	$7.8*10^{+4}$	$5*10^{-5}$	Blocks C3 activation by AP C3-convertase
C3-42.3	IgG2a	C3b, iC3b, C3c	MG4, MG5	0.73 nM	–	–	Blocks C3 activation by AP C3-convertase
C3-12.2	IgG1	iC3b, C3dg, C3d	CUB-TED	95 nM	$2.2*10^{+4}$	$2*10^{-5}$	na

deposition targets for opsonophagocytosis or direct destruction by initiating the lytic pathway, which triggers inflammation and formation of the membrane attack complex (MAC) [3]. The efficiency of complement activation relies on the AP amplification loop in which the C3b generated by the C3-convertase forms more AP C3-convertase and provides exponential amplification to the initial activation. In host, complement activation is strictly regulated and limited to the activator surface by a set of complement regulatory proteins in plasma and in the cellular surfaces [4].

C3 is the central protein in complement activation. It is involved in the most critical events of complement activation, which are the deposition of complement on activating surfaces and the amplification of the initial complement activation by the AP. Not surprisingly, C3 and its activated fragments are preferred therapeutic targets. Indeed, small molecules and monoclonal antibodies (mAbs) that inhibit C3 activation or block formation of the AP C3-convertase are considered the treatment of choice to prevent or ameliorate a long list of diseases in which dysregulation of the AP C3 convertase and C3 activation contributes to pathology by sustaining inflammation and perpetuating tissue damage [5–18]. In addition, because the covalent binding of C3 to complement activating surfaces is very stable, the identification of tissue-bound C3 activated fragments is routinely used as biomarker to reveal sites of complement activation.

Unfortunately, the repertoire of mAbs to C3 with potential therapeutic and diagnostic potential is limited, especially those that have been well characterized. Here we report the generation and complete functional and structural characterization of three novel mAbs that bind to C3 and block AP activation either by preventing C3 cleavage or inhibiting the assembly of the AP C3 convertase. These mAbs may offer novel therapeutic opportunities. We also describe one additional mAb that specifically recognizes iC3b, C3dg, and C3d. This last mAb reveals sites of on-going complement activation and thus could be used for targeted therapeutics or diagnostic purposes.

Results

Generation of mAbs targeting human C3, C3b, iC3b, and C3dg in mice

To generate monoclonal antibodies (mAbs) recognizing functionally relevant domains in C3 or its activated derivatives, we immunized C3-deficient female C57Bl/6 mice with a mixture of human C3b, iC3b, and C3dg fragments following standard procedures. The rationale behind the use of C3-deficient mice was to avoid tolerance towards the functionally relevant regions of human C3 fragments, which are likely those most evolutionary conserved. Hybridomas producing anti C3 mAbs were selected first based on their reactivity for C3 in ELISA, using a collection of purified proteins (C3, C3b, iC3b, C3c, and C3dg), and their capacity to inhibit AP-mediated lysis in a hemolysis assay using rabbit erythrocytes. Four clones (C3-16.4, C3-12.17, C3-42.3, and C3-12.2) were selected by these criteria (Table 1). C3-16.4, C3-12.17, and C3-42.3 recognize C3b, iC3b, and C3c and inhibit the lysis of rabbit erytrocytes in a dose-dependent way (Fig. 1A). They also completely block opsonization of the rabbit erythrocytes (Fig. 2). Importantly, the AP inhibitory mAbs achieved a 50% inhibition at approximately equimolar concentration with C3, thus strengthening the potential relevance of these mAbs as therapeutic agents. A fourth mAb C3-12.2 was selected because it specifically recognises iC3b, C3dg, and C3d.

The binding constants (KD) for C3 (C3-16.4, C3-12.17, and C3-42.3) and for iC3b (C3-12.2) were determined using Surface Plasmon Resonance (SPR; Biacore). All four mAbs showed KDs in the nM range (Table 1). We also tested the reactivity of these four mAbs in Western Blot (WB) and found that only C3-12.17 and C3-12.2 bind their targets (both, under reducing and non-reducing conditions) in this assay. C3-12.17 recognizes an epitope in the β chain (Fig. 1B and 1C) and C3-12.2 an epitope contained within C3d (see next section).

C3-12.2 specifically recognizes a neoepitope in iC3b that is preserved in C3d

C3-12.2 is the only of our four mAbs that does not recognise C3b in the ELISA assays. It binds to the α′65 chain of iC3b and the fragments resulting from iC3b cleavage, C3dg and C3d (Table 1). C3-12.2 does not bind to C3c, confirming that it does not recognise any region within the MG ring (Fig. 1C). We also observed that C3-12.2 also binds to C3d (Fig. 3A), which narrowed down the epitope recognized by the antibody to the C-terminal region of the C3d fragment, which is exposed only after C3b is cleaved by FI to generate iC3b. To confirm this result, we incubated either iC3b or C3d with the Fab fragment generated from C3-12.2 and analyzed the complex using single-molecule electron microscopy (EM) (Fig. 3B and C). Data generated were compared with those images

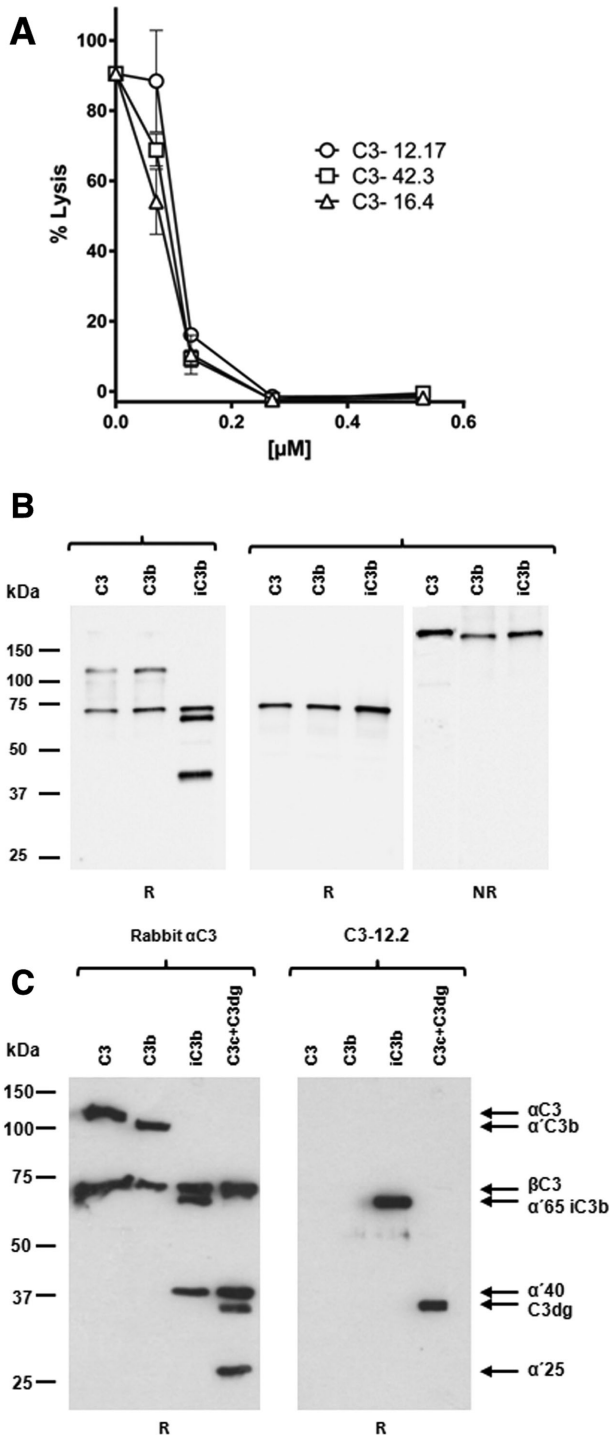

Figure 1. Screening and biochemical characterization of monoclonal antibodies. (A) Hemolytic assay using rabbit erythrocytes in the presence of NHS to determine the ability of C3-12.17, C3-42.3, and C3-16.4 to inhibit complement-mediated lysis. Data points represent mean ± SD of triplicate samples from one representative experiment out of three. (B) Detection of C3 fragments in western blot (WB) by the mAb C3-12.17 under reducing (R) and non-reducing conditions (NR). (C) Detection of C3 fragments in WB by C3-12.2 under reducing conditions (R). (B, C) Data shown are from a single experiment representative of four experiments performed.

obtained with the individual proteins. These analyses demonstrate the formation of C3d-Fab and iC3b-Fab complexes, confirming the location of interaction site of C3-12.2 in the TED domain of iC3b (Fig. 3B and C). The conclusion reached by single-molecule EM is also consistent with our results showing that C3-12.2 does not interfere with the inactivation of iC3b to C3dg by FI in the presence of Complement Receptor 1 (CR1) (Fig. 3D).

C3-12.2 demonstrated strong binding to SDS-denatured iC3b, C3dg, and C3d by WB analysis, but no detectable binding to SDS-denatured C3 or C3b (Fig. 1C). In addition, WB analysis using purified C3dg protein and activated plasma from human, mouse and rat also illustrated that the epitope recognized by mAb C3-12.2 is evolutionarily-conserved (Fig. 3E).

C3-12.17 and C3-42.3 inhibit the AP by blocking the interaction of C3 with the AP C3-convertase

C3-12.17 and C3-42.3 efficiently block AP-mediated opsonization and hemolysis of rabbit erythrocytes in the presence of normal human serum (Figs. 1A and 2). To determine at which level these mAbs inhibit the activation of the AP we performed in vitro experiments using purified C3, C3b, FB, and FD. In these experiments, C3, C3b and an equimolar mixture of C3 and C3b were incubated with FB and FD at 37°C for 15 min and the resulting activated fragments analyzed by SDS-PAGE under reducing conditions (Fig. 4). In the absence of inhibitory antibodies both, C3 and FB, are completely consumed, which is illustrated by the disappearance of the C3 α-chain and FB 90kDa bands and the generation of the C3 α'-chain and the Bb 60 kDa (Fig. 4). As expected, in the presence of C3-12.17 and C3-42.3 there was no activation of C3. However, FB was completely consumed, indicating that these two mAbs block activation of C3 but do not interfere the formation of the AP C3-convertase (Fig. 4). Thus, in the presence of C3-12.17 and C3-42.3, FB can bind C3b (or C3H2O) and FB is then efficiently cleaved by FD to the Bb and Ba fragments. Our interpretation was that C3-12.17 and C3-42.3 bind to the same region (or to two separate regions) in C3 and C3b that do not affect the binding of FB, but impair the interaction of the C3 with the AP C3-convertase, blocking the cleavage of the C3. Alternatively, these mAbs could block accessibility to the cleavage site in C3 by the catalytic site of the AP C3-convertase located in the Bb fragment.

Structural basis of the AP inhibition by C3-12.17 and C3-42.3

To understand the molecular basis of the inhibition of C3 activation by C3-12.17 and C3-42.3, we mapped the interaction site of C3-12.17 and C3-42.3 in C3 by resolving the 3D structure of the corresponding C3b-Fab complexes using single-molecule EM (Fig. 5). The Fab fragments from each of the two mAbs were generated following standard procedures and a molar excess of each Fab was then incubated with C3b. The C3b–Fab complexes were

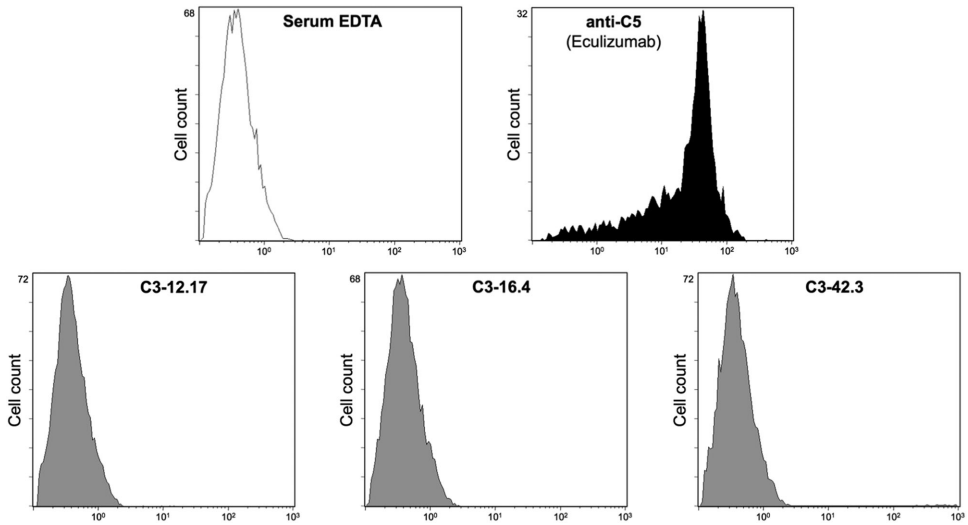

Figure 2. The mAbs C3-12.17, C3-16.4 and C3-42.3 inhibit C3 opsonization of rabbit erythrocytes. Rabbit erythrocytes were incubated with NHS and excess of the three different mAbs (C3-12.17, C3-16.4, and C3-42.3) and Eculizumab. NHS with EDTA was used as a negative control. Flow cytometry analysis using a rabbit polyclonal anti-C3 Ab was performed to detect the presence of C3 fragments. This experiment was performed in triplicate with identical results.

separated from the single components by size exclusion chromatography. Elution fractions from these gel filtration experiments were analyzed by SDS-PAGE to confirm the presence of the C3b–Fab complexes (Fig. 5A). The peak fraction containing the C3b–Fab complexes for each mAb was then analyzed using single-molecule EM. To this end, several thousand images of single molecules of the immune-complexes were extracted from the micrographs. 2D classification and image processing was used to calculate 2D averages with improved signal to noise ratio corresponding to several views of the complex, depending on the orientation of the molecules on the support film used for EM. Averages clearly revealed the presence of a Fab fragment bound to the MG

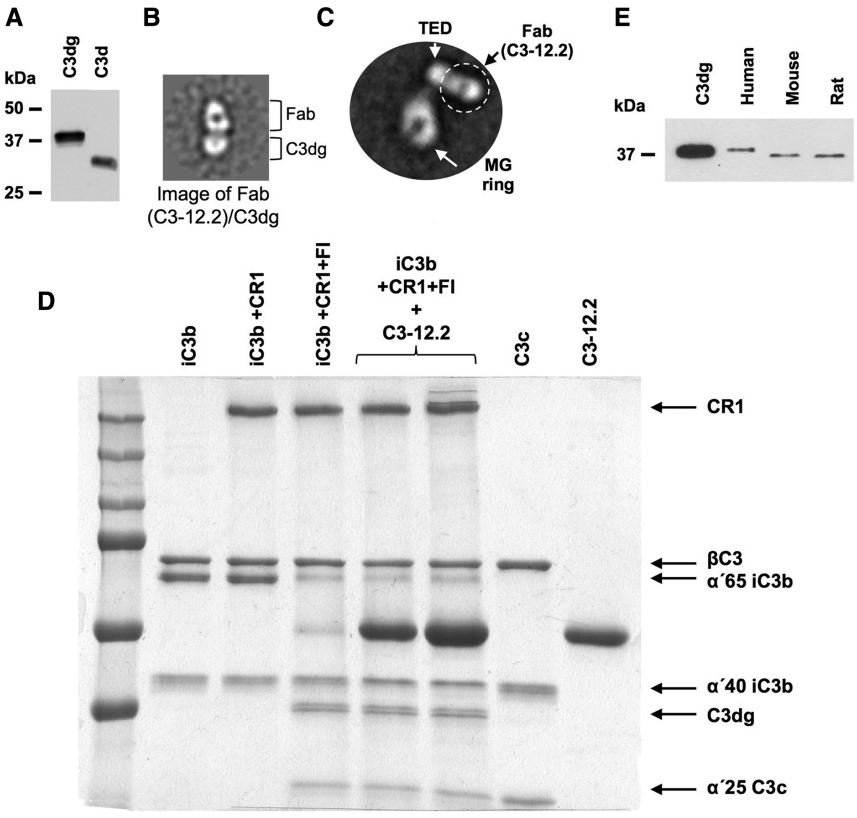

Figure 3. C3-12.2 recognizes an epitope in C3d exposed after cleavage of C3b to iC3b. (A) WB performed using purified proteins showing that C3-12.2 binds to the C3d epitope. (B) Electron microscopy average image of a Fab generated from C3-12.2 and its immune complex with C3d. The figure shows a representative 2D average of the Fab/C3d complex obtained after image processing of images obtained in the electron microscope. (C) Representative 2D average of the immune complex between C3-12.2 and iC3b. The position of the distinct domains was determined by comparison with previous EM structures from our group, and they are indicated. (D) C312.2 does not affect iC3b inactivation to C3dg in presence of CR1 and FI. Coomassie Blue staining of an in vitro reaction where iC3b was previously incubated with the C3-12.2 for 10′ at 37°C, and then, the CR1 and FI were added for another 60′ of incubation. The inactivation of iC3b is illustrated by the disappearance of the α′65 band and the generation of the C3dg band. (E) C3-12.2 recognizes the C3dg fragment in the activated plasma of human, mouse and rat, indicating that this mAb binds an evolutionary-conserved epitope in the C3dg molecule. Data shown are from a single experiment representative of three independent experiments.

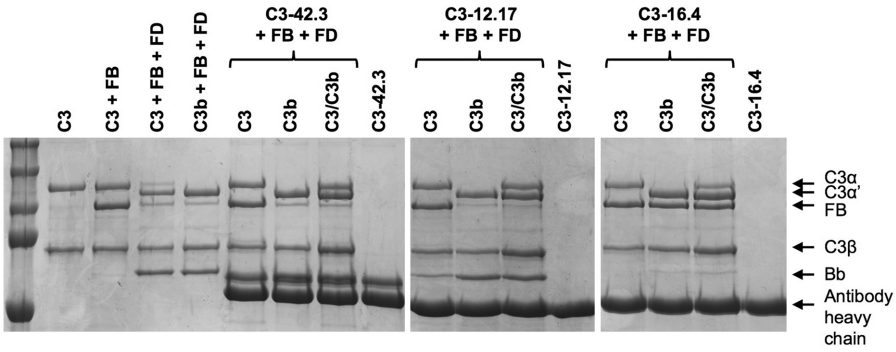

Figure 4. Functional effects of C3-12.17, C3-42.3, and C3-16.4 in C3 activation in vitro. In the presence of C3-12.17 and C3-42.3 there is no activation of C3, but FB is completely consumed. C3-16.4 blocks the activation of C3b and FB remains intact, suggesting that the mAb interferes with the assembly of the AP C3-convertase. All reactions were analyzed by Coomassie Blue staining. C3b was previously incubated with the different mAbs for 10′ at 37°C, and then, the FB and FD were added for another 45′of incubation. Data shown are form a single experiment representative of three independent experiments.

ring of C3b, but the positioning of the Fab was different for the C3-12.17 and C3-42.3 mAbs (Fig. 5B).

The precise location of the Fab in the each of the C3b–Fab complexes was defined more precisely by resolving the 3D structure of the complexes at 30 Å resolution using the single molecule images of the immune complexes as input for 3D refinement (Fig. 5C). The 3D structures were interpreted after fitting and combining the atomic structures of the MG ring from C3b, and a structure

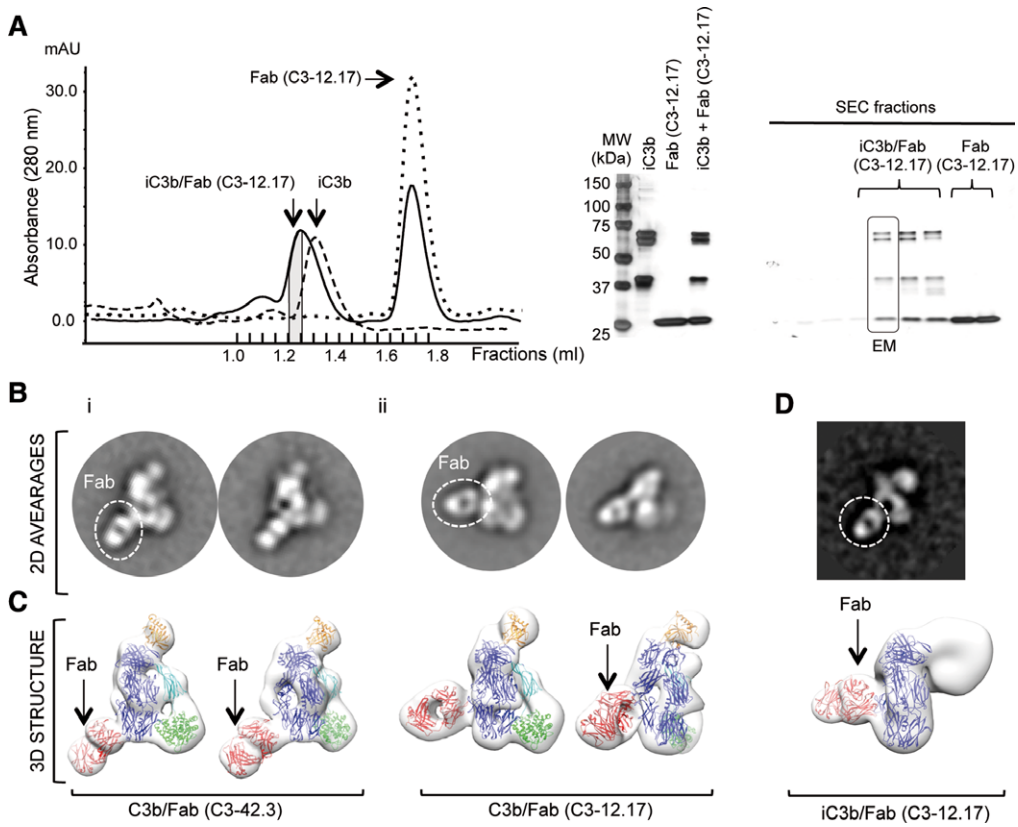

Figure 5. Purification and structure of immune-complexes for C3-42.3 and C3-12.17. (A) Fabs for each of these mAbs were incubated in molar excess with C3b or iC3b and the mixture was resolved by size-exclusion chromatography (SEC) (left panel). Figure shows only the chromatogram for the incubation of iC3b and Fab (C3-12.17) as a representative example. As control, each protein and Fab was also subjected to a SEC experiment before mixing. The immune complexes eluted first in the gel filtration column (continuous line) compared to C3b/iC3b (dashed line) and the Fab (dotted line). Fractions were analyzed by SDS-PAGE (right panel), and the peak fraction for the mixture containing both C3b/ic3b and the Fab was selected for structural analysis by electron microscopy (EM). This fraction is labeled in gray color in the chromatogram. (B) Representative 2D averages obtained after averaging several hundreds of images of complexes containing C3b and C3-42.3 (i) or C3-12.17 (ii), obtained in the electron microscope. The location of the Fab is indicated with a dashed white circle. (C) Two different views of the medium-resolution structure of the C3b/Fab complexes shown as a white transparent density. The structures were interpreted after fitting the crystal structures of C3b (PDB 2I07) [37] and a representative structure of a Fab. The MG ring is coloured in blue, TED domain in green, C345C in orange, and the Fab in red. (D) One representative average (top panel), and 3D structure (bottom panel) of Fab (C3-12.17) bound to iC3b. The location of the Fab is indicated within a dashed circle. In the structure, iC3b appears as in the conformation described in Alcorlo et al [38], and only the atomic structure of the MG ring and a Fab was fitted.

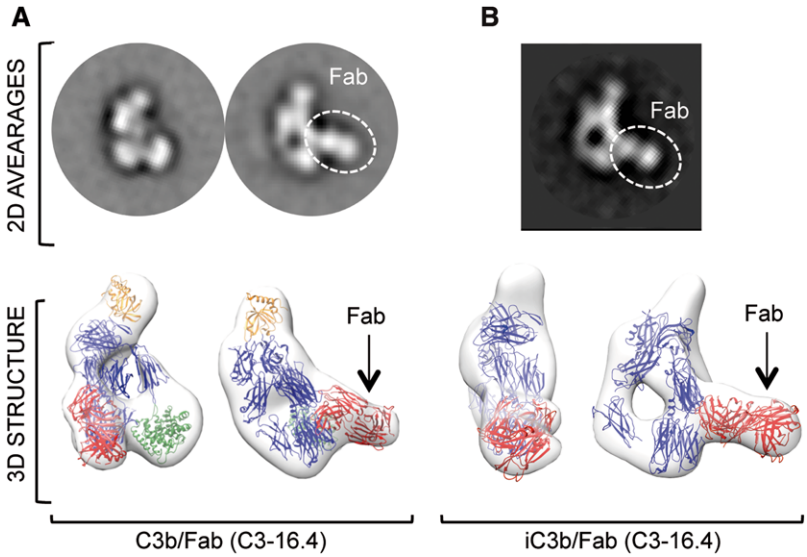

Figure 6. Structure of immune-complexes for C3-16.4. (A) Representative 2D averages obtained after averaging several hundreds of electron microscope images of complexes containing C3b and C3-16.4 (top). The location of the Fab is indicated with a dashed white circle. Two view of the medium-resolution structure of the C3b/Fab complex shown as a white transparent density (bottom). The structures were interpreted after fitting the crystal structures of C3b (PDB 2I07) [37] and a representative structure of a Fab. Color-coding as in Fig. 6. (B) One representative average (top), and 3D structure (bottom) of Fab (C3-16.4) bound to iC3b. The location of the Fab is indicated within a dashed circle. In the structure of iC3b, the TED domain is displaced in several positions on the EM images, and thus, its density is not observable after 2D and 3D averaging, as described before [39].

of a representative Fab, into the EM density, following standard methods used previously in our laboratory. As anticipated, the 3D structures revealed that C3-12.17 and C3-42.3 recognized two distinct positions of the MG ring. In both cases, the Fab fragment of the mAb projected from the MG outwards. Our models indicated that C3-12.17 recognizes a region around domains MG3 and MG4, whereas C3-42.3 binds to a region in the proximity of domains MG4 and MG5. These interaction sites are consistent with the binding specificity of C3-12.17 and C3-42.3 for C3b, iC3b, and C3c fragment, since all of these fragments contain the targeted epitopes in the MG ring (Table 1). Using similar methods, we analyzed the interaction of C3-12.17 with iC3b, finding, as expected, that C3-12.17 recognizes the same region in iC3b previously identified using C3b (Fig. 5D). As a whole, the resolution of the 3D structures of these C3b-Fab complexes explains how C3-12.17 and C3-42.3 block activation of C3 without affecting the assembly of the AP C3-convertase. These regions are distant from both the interaction site of FB and the cleavage site by the AP C3-convertase, demonstrating that C3-12.17 and C3-42.3 inhibit C3 activation by binding to a region of C3 and C3b that has been postulated to be involved in the recognition of the C3 substrate by the C3bBb AP C3-convertase [19–21].

C3-16.4 inhibits the AP by preventing the formation of the C3bBb C3-convertase

In contrast to C3-12.17 and C3-42.3 that inhibit C3 activation, but not the formation of the AP C3 convertase, C3-16.4 blocks the formation of the AP C3-convertase. In vitro experiments using purified C3, C3b, FB, and FD show that when these proteins are incubated together in the presence of C3-16.4 neither C3 and FB are consumed (Fig. 4). The inhibition of FB cleavage into Bb and Ba is particularly illustrative when C3b, FB, and FD are incubated together, as this indicates that C3-16.4 blocks formation of the AP C3-convertase (Fig. 4). Our conclusion from these data was that C3-16.4 inhibits AP activation by blocking the interaction of FB with C3b (or C3H20) and, therefore, the formation of the AP C3 convertase.

Structural basis of the AP inhibition by C3-16.4

Using a similar approach to that described before to map the binding site of C3-12.17 and C3-42.3 in C3, we have solved the 3D structure of the complexes formed between C3b (or iC3b)

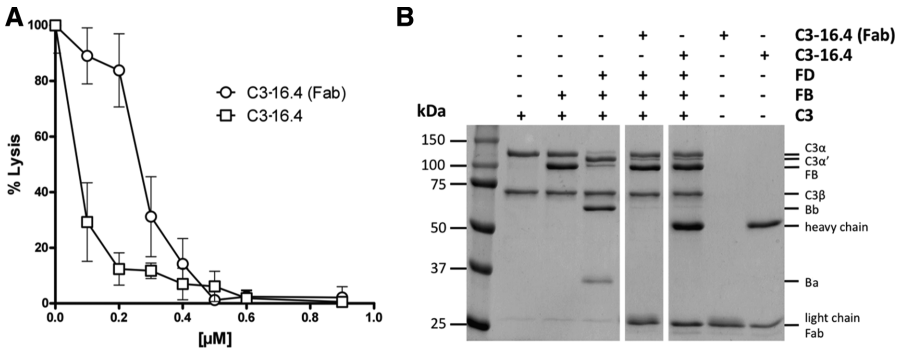

Figure 7. The C3-16.4 Fab fragment blocks the AP C3-convertase formation and prevents the complement mediated lysis of rabbit erythrocytes in presence of NHS. (A) Rabbit erythrocytes were incubated with NHS and increasing concentration of the C3-16.4 Ab or its Fab fragment. Data points represent mean ± SD of triplicate samples from one representative experiment out of three. (B) Coomassie-gel blue staining using purified proteins shows that the presence of either full C3-16.4 mAb or its Fab fragment prevent the cleavage of C3 or FB by the AP C3-convertase. Data shown are from a single experiment representative of three independent experiments.

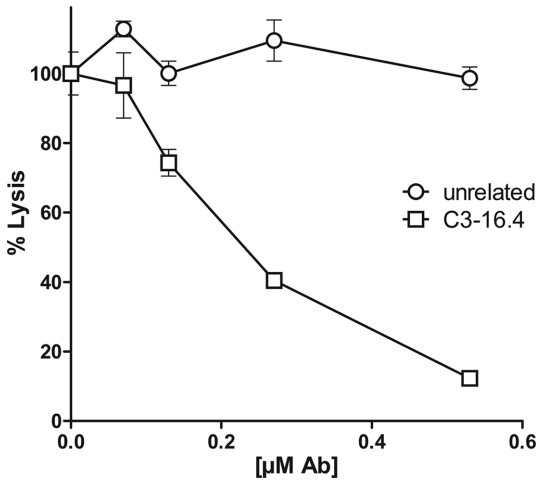

Figure 8. The C3-16.4 inhibits complement mediated lysis of rabbit erythrocytes in presence of mouse serum. Rabbit erythrocytes were incubated with 20% mouse serum and increasing concentration of the C3-16.4 mAb. Data points represent mean ± SD of triplicate samples from one representative experiment out of two.

with the Fab fragment of C3-16.4 (Fig. 6A and B). These data demonstrate that the C3-16.4 Fab recognizes a region around MG2 and MG6, and projects outward the C3b molecule. The region of C3 mapped by C3-16.4 is proximal, although not identical, to that mapped by H17, a humanized antibody that blocks FB binding to C3 and convertase formation [22]. C3-16.4 Fab sits proximal but not overlapping to regions in C3b involved in binding FB according to the structure of C3bB [23] (PDB 2XWJ). Thus, the effect of C3-16.4 on convertase formation must be indirect. A possibility could be that C3-16.4 alters the conformation of C3b in features essential for the binding to FB.

We were intrigued to know whether the inhibitory capacity of C3-16.4 is maintained in its Fab fragment or it is just a consequence of the large steric obstruction caused by the binding to C3b of the full antibody. Figure 7A illustrates that both full C3-16.4 and its Fab fragment efficiently inhibit the lysis of rabbit erythrocytes; the observed differences in the hemolytic assay likely being a consequence of the avidity effects on the surface of the rabbit erythrocytes. Using purified complement components we also show that both full C3-16.4 and its Fab fragment inhibit formation of the AP C3-convertase, blocking activation of FB and C3 (Fig. 7B).

C3-16.4 recognizes mouse C3 and efficiently blocks AP activation in mouse serum

Elisa assays using mouse serum demonstrated that C3-16.4, but not C3-12.17 and C3-42.3, recognizes mouse C3 and prevents the lysis of rabbit erytrocytes by mouse serum in a dose-dependent manner, achieving 50% blockage at equimolar C3:mAb concentrations (IC_{50}: 0.23 μM; [C3]: 0.3 μM) (Fig. 8). Binding constant (KD) of C3-16.4 for mouse C3 was calculated using SPR as KD = 6.8^{-8} (M), with Ka = 4.7^{+4} (1/Ms) and Kd = 3.2^{-4} (1/s) (Fig. 9). The KD value for mouse C3 is significantly different from that observed for human C3, which is basically due to the fact that C3-16.4 dissociates from mouse C3 very fast.

C3-12.17, C3-42.3, and C3-16.4 block complement-mediated lysis of sheep erythrocytes in in vitro

Atypical haemolytic uremic syndrome (aHUS) is characterized by impaired protection of endothelial cells from complement-mediated damage. In a significant numbers of aHUS patients, this impaired protection is a consequence of pathogenic variants in the complement factor H protein [24]. Complement dysregulation in aHUS sera can be demonstrated with a hemolytic assay using sheep erythrocytes [25] .Using an aHUS-like positive sera, consisting in a normal human serum depleted of 75% of its FH, we demonstrated that in this in vitro aHUS model the mAbs C3-12.17, C3-42.3 and C3-16.4 inhibit the lysis of the sheep erythrocytes in a concentration dependent fashion. Total inhibition of the lysis was achieved in all cases at concentration of the mAb that was essentially equimolar with that of serum C3 ([mAb]: 0.7 μM; [C3]: 0.83 μM) (Fig. 10).

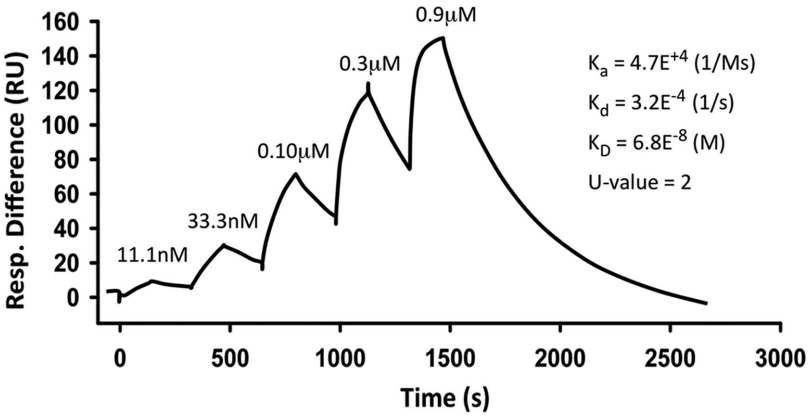

Figure 9. SPR analysis of binding of C3-16.4 mAb to mouse C3. The C3-16.4 mAb was captured using an anti-mouse IgG Ab surface and five increasing concentrations of mouse C3 were flowed over it. Data were fitted using 1:1 binding model. The resultant constants are shown at the right part of the panel. Data are from a single experiment with five samples.

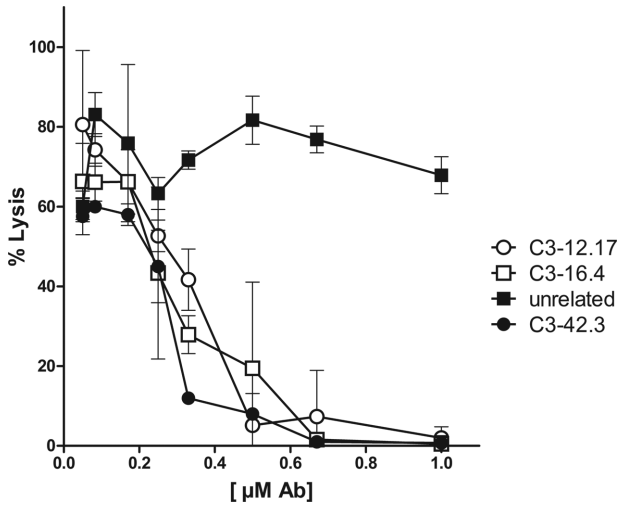

Figure 10. C3-12.17, C3-42.3 and C3-16.4 block the lysis of sheep erythrocytes in an in vitro aHUS model. Sheep erythrocytes were incubated in presence of 15% aHUS-like serum and increasing concentration of the mAbs (from 0.05 to 1 μM). An unrelated mAb was used as control. Data points represent mean ± SD of triplicate samples from one representative experiment out of three.

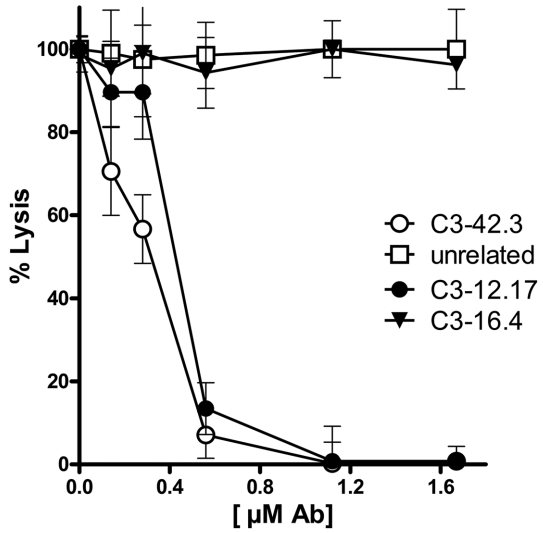

Figure 11. C3-12.17 and C3-42.3 efficiently prevent the lysis of PNH erythrocytes in acidified serum. Ham test with PNH erythrocytes was performed in the presence of increasing concentrations of the three mAbs. An unrelated mAb was used as a control. Data points represent mean ± SD triplicate samples from one representative experiment out of three.

C3-12.17 and C3-42.3 prevents lysis of PNH erythrocytes in acidified human serum

Paroxysmal nocturnal hemoglobinuria (PNH) is a rare complement-mediated hemolytic anemia characterized by the generation of erythrocytes lacking all GPI-anchored proteins, including the complement regulators CD55 and CD59, which are consequently susceptible to complement-mediate lysis [26]. The Ham test, a classical PNH assay [27], involves exposing the PNH erythrocytes to NHS acidified to pH 6.4 to initiate activation of the AP. We have performed the Ham test with PNH erythrocytes from an eculizumab-treated patient that are heavily opsonised with C3 fragments and demonstrate that addition of C3-12.17 and C3-42.3 efficiently block their lysis in a concentration-dependent fashion (Fig. 11). Total inhibition of the lysis in both cases was achieved at concentration of the mAbs that was essentially equimolar with that of C3 ([mAbs]: 0.92 μM; [C3]: 0.92 μM). Notably, the C3-16.4 fails to protect the lysis of C3-opsonized PNH erythrocytes, suggesting that this mAb does not prevent the formation of the AP C3-convertase when C3b is deposited on the cell surface. To test this possibility, we performed a haemolytic assay using rabbit erythrocytes that were heavy opsonized by incubating them with human serum in the presence of eculizumab.

The data replicate the results with the opsonized PNH erythrocytes showing that the mAb C3-16.4 does not protect the opsonized erythrocytes from lysis, whereas the mAb C3-12.17 does. These results support our conclusion that the mAb C3-16.4 does not block the AP C3-convertasa formation when C3b is deposited on the cell surfaces.

Discussion

Monoclonal antibodies (mAbs) against C3 and its activated fragments have many biomedical applications. They can be used to modulate the biological functions of C3, to target activated C3 fragments as *in vivo* delivery vehicles for new therapeutics or can be used as diagnostic agents to reveal sites of on-going complement activation [28]. These reagents are, however, scarce. We report here a detailed functional and structural characterization of four monoclonal antibodies (mAbs), generated by immunizing C3-deficient mice with a mixture of human C3b, iC3b, and C3dg fragments, which have these diagnostic and therapeutic potentialities. Three of these mAbs very efficiently inhibit activation of the AP. mAbs C3-12.17 and C3-42.3 bind to C3 and C3b with KDs in nM range (Table 1 and Figs. 1 and 2, and 4), which result in an almost irreversible binding to the target molecule at equimolar concentrations. WB analysis (Fig. 1) and 3D modeling using EM (Fig. 6) demonstrated that they recognize two distinct epitopes, both conserved in the C3/C3b/iC3b molecules, located close to each other within a region that have been postulated critical for the recognition of the C3 substrate by the AP C3 convertase (C3bBb) [19–21]. Binding of these mAbs to C3, or to C3b in the C3bBb convertase, efficiently blocks C3 activation (Figs. 1 and 2) and inhibits completely AP activation (Fig. 4). Our data also show that these mAbs do not interfere with the assembly of a C3bBb convertase (Fig. 4). In contrast, C3-16.4 and its Fab fragment bind to an epitope in a region of C3 around MG2-MG6 and impede the formation of the AP C3 proconvertase (C3bB) (Figs. 4 and 6).

C3-12.17, C3-42.3, and C3-16.4 are, therefore, new mAbs that can be added to the list of molecules able to block formation and/or activity of the AP C3-convertase and that, upon humanization could be used to down-modulate the AP in the long

list of diseases in which AP activation contributes to pathology. To provide proof of concept of the usefulness of the mAbs to prevent or ameliorate the consequences of complement activation in diseases characterized by AP complement dysregulation, we have used them successfully in an in vitro aHUS model with sheep erythrocytes (Fig. 10) and an ex vivo model using erythrocytes from PNH patients who are treated with eculizumab (Fig. 11). Eculizumab treatment has improved significantly the quality of life of PNH patients. However, because eculizumab does not block the activity of the AP C3 convertase, C3 opsonization of PNH erythrocytes persists, resulting in variable percentages of eythrocytes covered by C3 fragments, which are susceptible to extracellular hemolysis [29–31]. Using PNH erythrocytes obtained from patients treated with eculizumab, we were able to show that C3-12.17 and C3-42.3 efficiently prevented their lysis in the presence of acidified human serum (Fig. 11).

C3-12.17, C3-42.3, and C3-16.4 are distinct mAbs, targeting different epitopes in C3. Although these mAbs very efficiently inhibit the AP activity in human serum, the potential advantages of one of these mAbs over the others will require direct comparisons using in vivo models of disease, which we have not been able to address. C3-16.4 is the only of the three mAbs that recognizes both human and mouse C3. However, whilst binding of C3-16.4 to human C3 results in an almost irreversible binding, the binding of C3-16.4 to mouse C3 present a very high dissociation constant (Kd $= 3.2^{-4}$ (1/s)). This has prevented us from exploring the capacity of C3-16.4 to inhibit mouse complement in vivo in disease models generated in this species.

The structure/function correlations generated with the mAbs C3-12.17, C3-42.3 and C3-16.4 are also important because they provide additional support to the currently accepted 3D models that explain the assembly of the C3bBb convertase and the recognition of C3 by the C3bBb convertase. The attachment between two MG rings revealed by crystal structures of a dimeric convertase complex [21] and the crystal structure of cobra venom factor in complex with C5 [19] have been used to hypothesize how a convertase recognizes its substrate, C3. A mutation proximal to the proposed point of attachment between the convertase and C3 blocks substrate recognition by the convertase, supporting this model [20]. Our structural and functional analysis of mAbs C3-12.17 and C3-42.3 further strengthens this model. Both antibodies bind to the MG ring at a region that would prevent the formation of C3/C3b heterodimers, and as predicted by the current model, both mAbs do not block convertase formation but C3 cleavage to C3b is affected. On the other hand, C3-16.4 maps a region adjacent to that recognized by H17, a humanized antibody that blocks FB binding to C3b [22]. C3-16.4 interferes with the assembly of a convertase and the structural analysis suggests that these effects must be indirect, since the antibody does not bind to a region involved in the interaction with FB. A possibility could be that C3-16.4 modifies the conformation of C3b in aspects that are essential for the binding to FB.

In addition to the three antibodies that inhibit the AP activation, we report the generation and characterization of a fourth mAb C3-12.2 that specifically recognizes iC3b, C3dg, and C3d in human and several other species. This mAb can be used to target these activated C3 fragments in fluid phase or tissue-bound, which has both diagnostic and therapeutic importance. mAbs that recognize efficiently iC3b from different species are scarce and highly valuable because of their potential applications in clinical and basic research. C3-12.2, for example, was probed to be useful in detecting human and mouse iC3b/C3dg deposition over opsonized surfaces by flow cytometry and immunohistochemistry (data not shown), extending the small repertoire of mAbs that can be used to monitor complement activation [28]. Furthermore, C3-12.2 has also been successfully used in our laboratory to develop a specific ELISA to measure iC3b and to purify mouse C3dg to homogeneity from activated whole mouse serum using a single affinity chromatography step (data not shown).

In conclusion, mAbs targeting complement proteins are a continuous source of valuable reagents for the developing of therapeutic and diagnostic tools. They also provide insightful information to study structural functional relationships in complement activation and regulation. Despite the existence of other anti-complement mAbs, those that are well characterized in their functional and structural properties are not that common. In this respect, our four novel mAbs against human C3, added to those previously reported by Thurman *et al.* [28], offer a repertoire of novel reagents binding to functional regions or unique neo-epitopes in C3, with relevant diagnostic and therapeutic potentialities.

Materials and methods

Generation of monoclonal antibodies

C3-deficient mice were immunized with 20 μg of a mixture of the human activated C3 fragments, C3b, iC3b, and C3dg, emulsified in complete Freund's adjuvant. Subsequently, mice were boosted three times at 2-week intervals with the same amount of C3 fragments in incomplete adjuvant. The mice were screened for the development of antibodies to C3 by testing their sera in an ELISA using plates coated with equimolar amounts of the human C3 activated fragments. Positive mice were given an additional boost. Three days later spleen cells from a mouse having a robust immune response toward C3 were fused to the X63AG8 myeloma cell line. Candidate hybridomas were cloned by limiting dilution, and clones recognizing human activated C3 fragments were selected for further growing. mAbs from these hybridoma clones were purified from the supernatants by affinity chromatography using a protein-G sepharose column (Pharmacia, Uppsala, Sweden). The purity of the mAbs was then analyzed by 10 % SDS-PAGE and their immunoglobulin isotype determined with the IsoStrip Mouse Monoclonal Antibody Isotyping Kit (Roche Applied Science). All animal experimentation has been reviewed and approved by the CSIC Institutional Review Board (SAF2015-66287-R).

Isolation of complement components

C3 was purified from plasma EDTA using an established protocol [32]. C3b was generated by C3-convertase cleavage. iC3b was produced by incubation of C3b in presence of FH and FI in Hepes 10 mM, NaCl 150 mM, whereas C3dg was produced by incubation of C3b with FH and FI at low ionic strength. iC3b and C3dg were purified by anion exchange and size exclusion chromatography. FD was purchased from Calbiochem. Concentrations of pure C3 and C3 activated fragments were assessed using absorbance at A280 and a extinction coefficients of 0.98 cm^{-1} $(mg/mL)^{-1}$.

ELISAs

To characterize the reactivity of the antibodies against the different C3 fragments we performed a direct ELISA coating the plates with purified human C3, C3b, iC3b and C3dg or mouse C3 at 1 μg/ml ON at 4°C in PBS pH 7.4. After blocking with BSA, increasing amounts of the antibodies were added (0.5 to 2 μg/mL) and detected with a HRP-conjugated anti-mouse IgG (1:1000).

Inhibition of C3 cleavage assay

To test the ability of the mAbs to inhibit C3 cleavage we used an in vitro assay using purified C3 (1 μg), FB (1 μg) and FD (5 ng) components in 25 uL of AP buffer (2.9 mM barbital, 1.7 mM sodium barbital, 144 mM NaCl, 7 mM $MgCl_2$, 10 mM EGTA, pH 7.4). The C3 was first incubated in presence of 2 μg and 4 μg of each mAb for 10 min at 37 °C in a water bath. Then, the FB was added and 10 min later FD, allowing the reaction to proceed for 40 min longer. Cleavage of C3 was assessed in 10% SDS-PAGE under reducing conditions and Coomassie blue staining.

Hemolytic assays

The capacity of the mAbs to prevent the activation of AP on cellular surfaces was assessed with the classical AP hemolytic assay using rabbit erythrocytes as previously described [33], and the hemolytic assay using sheep erythrocytes to test sera from atypical uremic syndrome(aHUS) patients [25]. For this assay, we used an aHUS-like serum consisting of a normal human serum that has been depleted of 75% of the FH. For the haemolytic assay using mouse serum, the mouse serum concentration was 20%.

Rabbit erythrocytes were also used to test the capacity of the mAbs to prevent C3 deposition on cell surfaces. Briefly, 100 μL of rabbit erythrocytes (1×10^8/mL) in AP buffer were incubated with 5 % NHS in presence of either Eculizumab (Soliris®, Alexion Pharmaceuticals) or the different mAbs against C3 at 37°C for 30 min. C3 deposition was evaluated by flow cytometry using a rabbit polyclonal anti human C3 antibody (in house; 1 μg/mL in PBS).

To test the capacity of the mAbs to inhibit acidified lysis of PNH erythrocytes (the Ham test) [27], we incubated at 37°C for 1h PNH erythrocytes (4 % v:v final) with 25 % NHS in AP buffer acidified by addition of 9 % of HCl 0.2 M, in the presence of increasing amounts of the mAbs. Hemolysis in supernatants was read at 540 nm and the percentage of lysis calculated using zero and 100 % lysis controls.

Generation of Fabs from purified mAbs

Fabs were produced using Pierce® Mouse IgG_1 Fab and $F(ab')_2$ Preparation Kit (Thermo Scientific) according to the instructions provided by the manufacturer. The Fabs were purified using size-exclusion chromatography and a Superdex 200 (GE Healthcare) in 20 mM Tris, 60 mM, 1% EDTA-free protease inhibitor (Roche). The peak fractions were concentrated using Amicon® Ultra-4 Centrifugal Filter Units (Millipore) and analyzed by SDS-PAGE to verify the presence of the Fab.

Determination of binding constants (KD) by surface plasmon resonance (SPR)

All SPR analyses were carried out on a Biacore X100 (GE Healthcare). For the determination of binding constants (KD) of the mAbs we used a single-cycle-kinetics method. This approach consisted of five consecutive injections of C3b or mouse C3 (analyte) at increasing concentrations, over a surface in which the mAbs were captured using an anti-mouse antibody as described previously [33]. Each injection lasted for 150 s separated by a dissociation period of 180 s, during which C3-free buffer was injected. The cycle was completed with an extended dissociation period of 3900 s and a regeneration step to release both the anti-C3 mAbs and C3.

Electron microscopy and 3D reconstruction of immune complexes

Immune complexes were prepared by mixing a 1.5 to 3.0 molar excess of Fab with C3b or iC3b, incubated for 30 min at 37°C and then diluted and adsorbed on carbon-coated grids for negative staining with 1% uranyl formate. Imaging was performed in a JEOL-1230 100 kV and data automatically acquired with a TVIPS F416 CMOS at 54926 of final magnification. Automated particle selection as implemented in EMAN2 [34] was used to select >15 000 particles per experiment and then classified and averaged in XMIPP [34]. Initial models were generated in EMAN2 or created directly from a C3b atomic structure (PDB 2I07). 3D structures were refined in XMIPP [35] reaching an estimated resolution of 29–30 Å in all cases following the FSC 0.5 criteria. Fitting of atomic structures was performed using UCSF Chimera [36]. In the case of the complexes between C3-12.2 and iC3b a similar strategy was followed, but the heterogeneity of the C3d domain location limited the analysis to 2D classification and averaging.

Acknowledgements: Work in this report has been funded by the Spanish "Ministerio de Economía y Competitividad" (SAF2011-26583 and SAF2015-66287-R to SRdC and SAF2014-52301-R to OL) and the Seventh Framework Programme European Union Project EURenOmics (305608) to SRdC. In addition, this work has been supported by a grant from the Autonomous Region of Madrid (S2010/BMD-2316) to SRdeC and OL.

Conflict of interest: The authors declare no financial or commercial conflict of interest.

References

1 **Walport, M. J.**, Complement. First of two parts. *N. Engl. J. Med.* 2001. **344**: 1058–1066.

2 **Walport, M. J.**, Complement. Second of two parts. *N. Engl. J. Med.* 2001. **344**: 1140–1144.

3 **Morgan, B. P.**, Regulation of the complement membrane attack pathway. *Crit. Rev. Immunol.* 1999. **19**: 173–198.

4 **Lachmann, P. J.**, The amplification loop of the complement pathways. *Adv. Immunol.* 2009. **104**: 115–149.

5 **Holers, V. M. and Thurman, J. M.**, The alternative pathway of complement in disease: opportunities for therapeutic targeting. *Mol. Immunol.* 2004. **41**: 147–152.

6 **Thurman, J. M., Kraus, D. M., Girardi, G., Hourcade, D., Kang, H. J., Royer, P. A., Mitchell, L. M. et al.**, A novel inhibitor of the alternative complement pathway prevents antiphospholipid antibody-induced pregnancy loss in mice. *Mol. Immunol.* 2005. **42**: 87–97.

7 **DiLillo, D. J., Pawluczkowycz, A. W., Peng, W., Kennedy, A. D., Beum, P. V., Lindorfer, M. A. and Taylor, R. P.**, Selective and efficient inhibition of the alternative pathway of complement by a mAb that recognizes C3b/iC3b. *Mol. Immunol.* 2006. **43**: 1010–1019.

8 **Leinhase, I., Rozanski, M., Harhausen, D., Thurman, J. M., Schmidt, O. I., Hossini, A. M., Taha, M. E. et al.**, Inhibition of the alternative complement activation pathway in traumatic brain injury by a monoclonal anti-factor B antibody: a randomized placebo-controlled study in mice. *J. Neuroinflammation* 2007. **4**: 13.

9 **Katschke, K. J., Jr., Stawicki, S., Yin, J., Steffek, M., Xi, H., Sturgeon, L., Hass, P. E. et al.**, Structural and functional analysis of a C3b-specific antibody that selectively inhibits the alternative pathway of complement. *J. Biol. Chem.* 2009. **284**: 10473–10479.

10 **Lindorfer, M. A., Pawluczkowycz, A. W., Peek, E. M., Hickman, K., Taylor, R. P. and Parker, C. J.**, A novel approach to preventing the hemolysis of paroxysmal nocturnal hemoglobinuria: both complement-mediated cytolysis and C3 deposition are blocked by a monoclonal antibody specific for the alternative pathway of complement. *Blood* 2010. **115**: 2283–2291.

11 **Risitano, A. M., Notaro, R., Pascariello, C., Sica, M., del Vecchio, L., Horvath, C. J., Fridkis-Hareli, M. et al.**, The complement receptor 2/factor H fusion protein TT30 protects paroxysmal nocturnal hemoglobinuria erythrocytes from complement-mediated hemolysis and C3 fragment. *Blood* 2012. **119**: 6307–6316.

12 **Katschke, K. J., Jr., Wu, P., Ganesan, R., Kelley, R. F., Mathieu, M. A., Hass, P. E., Murray, J. et al.**, Inhibiting alternative pathway complement activation by targeting the factor D exosite. *J. Biol. Chem.* 2012. **287**: 12886–12892.

13 **Zhang, Y., Nester, C. M., Holanda, D. G., Marsh, H. C., Hammond, R. A., Thomas, L. J., Meyer, N. C. et al.**, Soluble CR1 therapy improves complement regulation in C3 glomerulopathy. *J. Am. Soc. Nephrol.* 2013. **24**: 1820–1829.

14 **Risitano, A. M., Ricklin, D., Huang, Y., Reis, E. S., Chen, H., Ricci, P., Lin, Z. et al.**, Peptide inhibitors of C3 activation as a novel strategy of complement inhibition for the treatment of paroxysmal nocturnal hemoglobinuria. *Blood* 2014. **123**: 2094–2101.

15 **Nichols, E. M., Barbour, T. D., Pappworth, I. Y., Wong, E. K., Palmer, J. M., Sheerin, N. S., Pickering, M. C. et al.**, An extended mini-complement factor H molecule ameliorates experimental C3 glomerulopathy. *Kidney Int.* 2015. **88**: 1314–1322.

16 **Mastellos, D. C., Yancopoulou, D., Kokkinos, P., Huber-Lang, M., Hajishengallis, G., Biglarnia, A. R., Lupu, F. et al.**, Compstatin: a C3-targeted complement inhibitor reaching its prime for bedside intervention. *Eur. J. Clin. Invest.* 2015. **45**: 423–440.

17 **Mastellos, D. C., Reis, E. S., Yancopoulou, D., Hajishengallis, G., Ricklin, D. and Lambris, J. D.**, From orphan drugs to adopted therapies: advancing C3-targeted intervention to the clinical stage. *Immunobiology* 2016. **221**: 1046–1057.

18 **Ricklin, D. and Lambris, J. D.**, New milestones ahead in complement-targeted therapy. *Semin. Immunol.* 2016. **28**: 208–222.

19 **Laursen, N. S., Andersen, K. R., Braren, I., Spillner, E., Sottrup-Jensen, L. and Andersen, G. R.**, Substrate recognition by complement convertases revealed in the C5-cobra venom factor complex. *Embo. J.* 2011. **30**: 606–616.

20 **Martinez-Barricarte, R., Heurich, M., Valdes-Canedo, F., Vazquez-Martul, E., Torreira, E., Montes, T., Tortajada, A. et al.**, Human C3 mutation reveals a mechanism of dense deposit disease pathogenesis and provides insights into complement activation and regulation. *J. Clin. Invest.* 2010. **120**: 3702–3712.

21 **Rooijakkers, S. H., Wu, J., Ruyken, M., van Domselaar, R., Planken, K. L., Tzekou, A., Ricklin, D. et al.**, Structural and functional implications of the alternative complement pathway C3 convertase stabilized by a staphylococcal inhibitor. *Nat. Immunol.* 2009. **10**: 721–727.

22 **Paixao-Cavalcante, D., Torreira, E., Lindorfer, M. A., Rodriguez de Cordoba, S., Morgan, B. P., Taylor, R. P., Llorca, O. et al.**, A humanized antibody that regulates the alternative pathway convertase: potential for therapy of renal disease associated with nephritic factors. *J. Immunol.* 2014. **192**: 4844–4851.

23 **Forneris, F., Ricklin, D., Wu, J., Tzekou, A., Wallace, R. S., Lambris, J. D. and Gros, P.**, Structures of C3b in complex with factors B and D give insight into complement convertase formation. *Science* 2010. **330**: 1816–1820.

24 **Rodriguez de Cordoba, S., Hidalgo, M. S., Pinto, S. and Tortajada, A.**, Genetics of atypical hemolytic uremic syndrome (aHUS). *Semin. Thromb. Hemost.* 2014. **40**: 422–430.

25 **Sanchez-Corral, P., Gonzalez-Rubio, C., Rodriguez de Cordoba, S. and Lopez-Trascasa, M.**, Functional analysis in serum from atypical Hemolytic Uremic Syndrome patients reveals impaired protection of host cells associated with mutations in factor H. *Mol. Immunol.* 2004. **41**: 81–84.

26 **Risitano, A. M.**, Paroxysmal nocturnal hemoglobinuria and other complement-mediated hematological disorders. *Immunobiology* 2012. **217**: 1080–1087.

27 **Ham, T. H. and Dingle, J. H.**, Studies on destruction of red blood cells.II. Chronic hemolytic anemia with paroxysmal nocturnal hemoglobinuria:certain immunological aspects of the hemolytic mechanism with special reference to serum complement. *J. Clin. Invest.* 1939. **18**: 657–672.

28 **Thurman, J. M.**, **Kulik, L.**, **Orth, H.**, **Wong, M.**, **Renner, B.**, **Sargsyan, S. A.**, **Mitchell, L. M. et al.**, Detection of complement activation using monoclonal antibodies against C3d. *J. Clin. Invest.* 2013. **123**: 2218–2230.

29 **Risitano, A. M.**, **Notaro, R.**, **Marando, L.**, **Serio, B.**, **Ranaldi, D.**, **Seneca, E.**, **Ricci, P. et al.**, Complement fraction 3 binding on erythrocytes as additional mechanism of disease in paroxysmal nocturnal hemoglobinuria patients treated by eculizumab. *Blood* 2009. **113**: 4094–4100.

30 **Hill, A.**, **Rother, R. P.**, **Arnold, L.**, **Kelly, R.**, **Cullen, M. J.**, **Richards, S. J. and Hillmen, P.**, Eculizumab prevents intravascular hemolysis in patients with paroxysmal nocturnal hemoglobinuria and unmasks low-level extravascular hemolysis occurring through C3 opsonization. *Haematologica* 2010. **95**: 567–573.

31 **Lin, Z.**, **Schmidt, C. Q.**, **Koutsogiannaki, S.**, **Ricci, P.**, **Risitano, A. M.**, **Lambris, J. D. and Ricklin, D.**, Complement C3dg-mediated erythrophagocytosis: implications for paroxysmal nocturnal hemoglobinuria. *Blood* 2015. **126**: 891–894.

32 **Montes, T.**, **Tortajada, A.**, **Morgan, B. P.**, **Rodriguez de Cordoba, S. and Harris, C. L.**, Functional basis of protection against age-related macular degeneration conferred by a common polymorphism in complement factor B. *Proc. Natl. Acad. Sci. U. S. A.* 2009. **106**: 4366–4371.

33 **Subias, M.**, **Tortajada, A.**, **Gastoldi, S.**, **Galbusera, M.**, **Lopez-Perrote, A.**, **Lopez Lde, J.**, **Gonzalez-Fernandez, F. A. et al.**, A novel antibody against human factor B that blocks formation of the C3bB proconvertase and inhibits complement activation in disease models. *J. Immunol.* 2014. **193**: 5567–5575.

34 **Tang, G.**, **Peng, L.**, **Baldwin, P. R.**, **Mann, D. S.**, **Jiang, W.**, **Rees, I. and Ludtke, S. J.**, EMAN2: an extensible image processing suite for electron microscopy. *J. Struct. Biol.* 2007. **157**: 38–46.

35 **Sorzano, C. O.**, **Marabini, R.**, **Velazquez-Muriel, J.**, **Bilbao-Castro, J. R.**, **Scheres, S. H.**, **Carazo, J. M. and Pascual-Montano, A.**, XMIPP: a new generation of an open-source image processing package for electron microscopy. *J. Struct. Biol.* 2004. **148**: 194–204.

36 **Goddard, T. D.**, **Huang, C. C. and Ferrin, T. E.**, Visualizing density maps with UCSF Chimera. *J. Struct. Biol.* 2007. **157**: 281–287.

37 **Janssen, B. J.**, **Christodoulidou, A.**, **McCarthy, A.**, **Lambris, J. D. and Gros, P.**, Structure of C3b reveals conformational changes that underlie complement activity. *Nature* 2006. **444**: 213–216.

38 **Alcorlo, M.**, **Martinez-Barricarte, R.**, **Fernandez, F. J.**, **Rodriguez-Gallego, C.**, **Round, A.**, **Vega, M. C.**, **Harris, C. L. et al.**, Unique structure of iC3b resolved at a resolution of 24 A by 3D-electron microscopy. *Proc. Natl. Acad. Sci. U. S. A.* 2011. **108**: 13236–13240.

39 **Chen, X.**, **Yu, Y.**, **Mi, L. Z.**, **Walz, T. and Springer, T. A.**, Molecular basis for complement recognition by integrin alphaXbeta2. *Proc. Natl. Acad. Sci. U. S. A.* 2012. **109**: 4586–4591.

Full correspondence: Prof. Oscar Llorca
e-mail: ollorca@cib.csic.es

Additional correspondence: Prof. Santiago Rodríguez de Córdoba, Centro de Investigaciones Biológicas, Ramiro de Maeztu 9, 28040 Madrid, Spain
e-mail: srdecordoba@cib.csic.es

Received: 11/10/2016
Revised: 15/12/2016
Accepted: 11/1/2017
Accepted article online: 13/1/2017

